EFFECT OF MICROSTRUCTURAL DAMAGE ON ULTRASONIC VELOCITY AND ELASTIC MODULI OF PARTIALLY STABILIZED ZIRCONIA

Wayne P. Rogers, Jon Isaacs, and S. Nemat-Nasser

Center of Excellence for Advanced Materials
Department of Applied Mechanics and Engineering Sciences
University of California, San Diego
La Jolla, CA 92093

INTRODUCTION

Zirconia toughened ceramics, such as magnesia partially stabilized zirconia (Mg-PSZ), have received considerable attention due to their high strength and fracture toughness [1]. These properties are a consequence of stress-induced microstructural changes which inhibit crack propagation and provide a degree of 'damage tolerance' not common to other ceramic materials. Ultrasonic testing can aid in the characterization of microstructural changes associated with transformation plasticity [2]. The present paper presents measurements of ultrasonic velocity as a function of microstructural damage in Mg-PSZ loaded in compression at high strain rates. Observed changes in elastic moduli are compared to a model of a solid containing randomly distributed penny-shaped microcracks which are all oriented parallel to the axis of compression.

STRESS-INDUCED MICROSTRUCTURAL DAMAGE IN MG-PSZ

Samples were tested with a Split Hopkinson Pressure Bar [3] modified for ceramic materials to accurately measure small sample strains. Instead of the traditional technique, the strain was measured directly from a strain gauge on the sample itself. The strain rate was controlled by placing a small copper tab between the striker bar and the incident bar. Plastic deformation of the copper tab resulted in a triangular shaped input pulse to the sample. The strain rate was 250 /s. Stress in the sample was measured in the traditional way, i.e., from the strain pulse in the transmitter bar. The Mg-PSZ* has a 50 μm grain size and a density of 5.7 g/cc. A sample size of 0.25" x 0.25" the transverse directions and 0.32" in the axial direction was used.

Fig.1 shows the stress-strain curve for Mg-PSZ obtained in the Split Hopkinson Pressure Bar tests. The initial elastic modulus is 200 GPa. The sample was loaded once to a maximum stress of 1.76 GPa and then reloaded to a maximum stress of 2.03 GPa. The material exhibits considerable inelastic deformation when loaded in compression, with a 'yield' stress of roughly 1.2 GPa. The permanent axial strains after the two tests are 0.09% and 0.36%. It has been shown [2] that the mechanisms of plastic deformation in Mg-PSZ are: 1) a volumetric expansion associated with the stress induced phase transformation; 2) shear

* MS-grade ZrO_2, Nilcra Ceramics Inc., St. Charles, IL.

strains from the formation of shear bands within transformed grains; and 3) dilatational strains due to microcracking. Four levels of maximum compressive strain are identified in Fig.1: level A, the initial condition; level B, shortly after the onset of plastic deformation; level C, at intermediate plastic deformation; and level D, near the maximum strain prior to final failure.

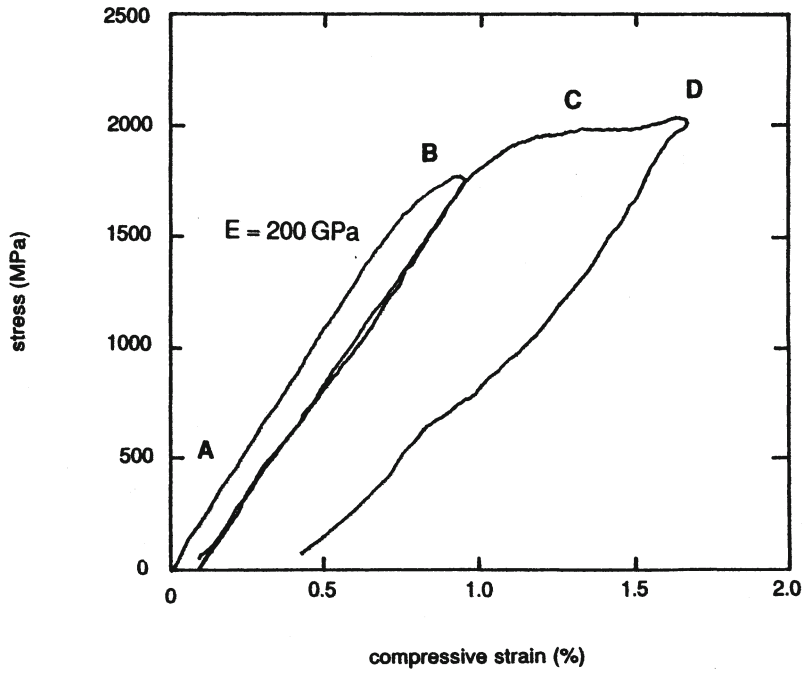

Fig. 1. Stress-strain curve for Mg-PSZ measured in the Split Hopkinson Pressure Bar modified for ceramics.

Optical micrographs of polished free surfaces of samples at levels B and C are shown in Figs. 2 and 3. Nomarski interference highlights the surface distortions caused by transformation strains of preferentially oriented grains. The higher magnification photographs show porosity, polishing marks, and distortions of individual grains. More surface distortion occurs at higher strain (Fig. 3) as the volume fraction transformed increases. Microcracks, roughly the size of grains, are apparent. The cracks are distributed uniformly over the free surface and oriented parallel to the compression loading axis. At damage level D (not shown) the size of microcracks remains roughly constant but the density of cracks increases.

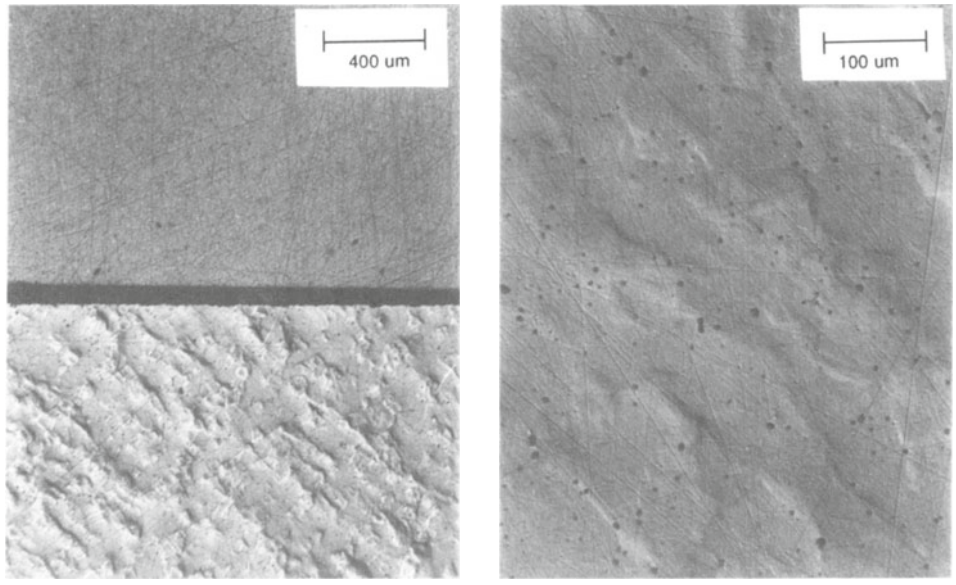

Fig. 2. Mg-PSZ stressed in the Hopkinson Pressure Bar. Compression axis is horizontal. Top left: initial condition; bottom left: strain level B, 0.8%; right: higher magnification.

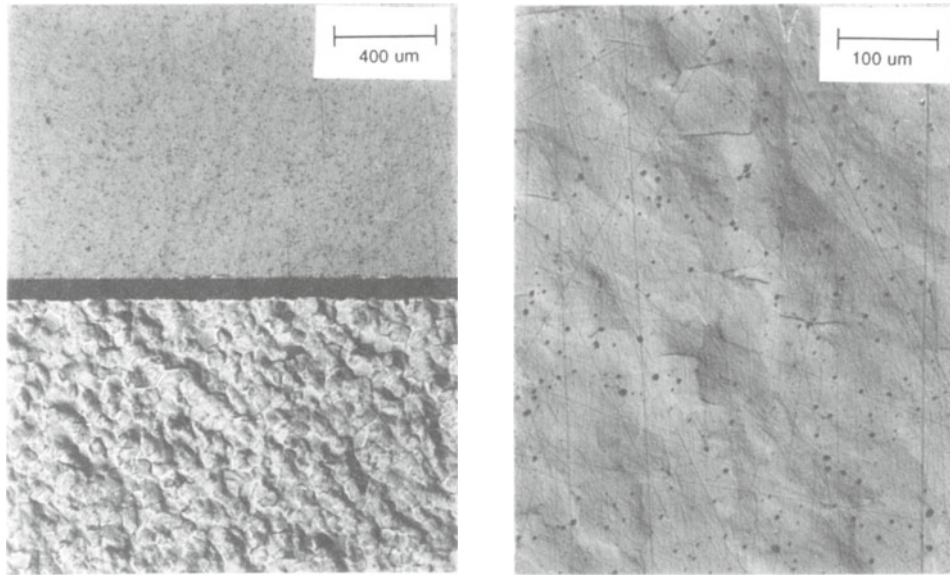

Fig. 3. Mg-PSZ stressed in the Hopkinson Pressure Bar. Compression axis is horizontal. Top left: initial condition; bottom left: strain level C, 1.2%; right: higher magnification.

ULTRASONIC VELOCITY

Ultrasonic velocity was measured in samples subjected to varying levels of plastic deformation. Longitudinal and shear wave velocities were measured in two directions: parallel to the compression loading axis and transverse to the loading axis. The pulse-echo-overlap method [4] was used to measure transit time. Attenuation was much higher in samples with higher levels of plastic deformation but three echoes could be detected in all cases. Figs. 4 and 5 show the longitudinal and shear wave velocities as a function of the maximum compressive strain the samples experienced in the Hopkinson Bar test. Strain levels A, B, C and D are identified. In the initial condition, A, there is a small anisotropy evident from the difference between the velocities in the axial and transverse directions. The longitudinal wave velocity in the axial direction is not strongly affected by compression induced microstructural changes. However, in the transverse direction the longitudinal wave velocity decreases dramatically at level D. There is

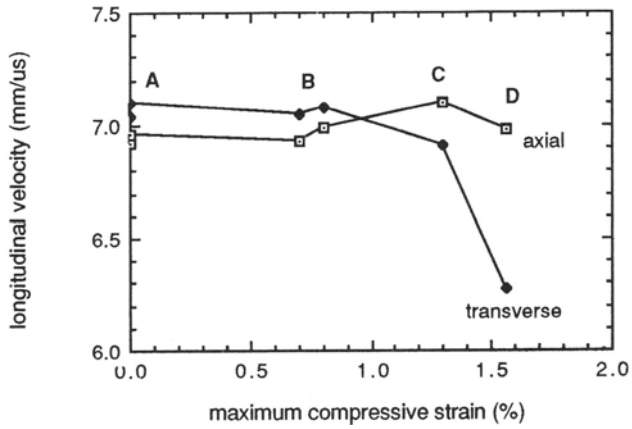

Fig. 4. Longitudinal wave velocity in Mg-PSZ after testing in the Hopkinson Pressure Bar.

evidence that the decrease in longitudinal wave velocity is due to microcracking parallel to the axis of compression in the material. First, the decrease begins at a strain level which coincides with the onset of visible microcracks on the free surface of the sample. Furthermore, the microcracks would not be expected to affect the longitudinal wave velocity in the axial direction, since the cracks are oriented parallel to the loading axis. Fig. 5 shows that the shear wave velocity in the axial direction is not affected strongly by the compression-induced microstructural changes. In the transverse direction the shear wave velocity increases at intermediate strain levels followed by a moderate decrease at higher levels. The increase may be due to an increase in the shear stiffness. Microcracking may be responsible for the decrease in shear wave velocity at high microstructural damage levels.

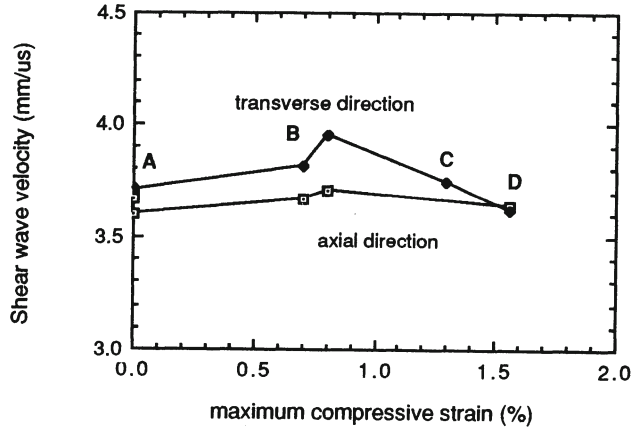

Fig. 5. Shear wave velocity in Mg-PSZ after testing in the Hopkinson Pressure Bar.

ELASTIC MODULI OF A CRACKED SOLID

Analytical expressions for the elastic moduli of solids containing distributed microcracks have been developed by several researchers. Budiansky and O'Connell [5] treat the case of flat elliptical cracks randomly distributed in an isotropic homogeneous medium. Horii and Nemat-Nasser [6] consider microcracking induced anisotropy. A solid containing cracks oriented parallel to one axis is transversely isotropic. There are several ways in which the corresponding elastic moduli can be estimated. In the self-consistent method, a crack is embedded in a homogeneous elastic solid whose overall moduli is sought. This requires calculating the crack opening displacement for an elliptical crack in an anisotropic material. When the density of the microcracks is relatively small, one may use a much simpler technique, by embedding a penny-shaped crack in the isotropic linearly elastic matrix, and hence, neglecting the interaction effects. In this case we can follow the method of Nemat-Nasser [7] and obtain, for penny-shaped cracks parallel to the axis of compression but having random orientations normal to this direction, the effective elastic moduli in a direction normal to the axis of symmetry,

$$\frac{\bar{E}}{E} = \left\{1 + \varepsilon\frac{2(1-\nu^2)(8-3\nu)}{3(2-\nu)}\right\}^{-1} \tag{1}$$

$$\frac{\bar{\nu}}{\nu} = \left\{1 + \varepsilon\frac{2(1-\nu^2)}{3(2-\nu)}\right\}\left\{1 + \varepsilon\frac{2(1-\nu^2)(8-3\nu)}{3(2-\nu)}\right\}^{-1} \tag{2}$$

$$\frac{\bar{\mu}}{\mu} = \left\{1 + \varepsilon\frac{4(1-\nu)(4-\nu)}{3(2-\nu)}\right\}^{-1} \tag{3}$$

where E, μ and ν are the Young's modulus, shear modulus and Poisson's ratio, respectively, of the matrix, $\bar{E}$, $\bar{\mu}$ and $\bar{\nu}$ refer to the cracked material, and ε is a crack density parameter, $\varepsilon = N\langle a^3\rangle$ for circular cracks of radius a; here N is the density of cracks per unit volume, and the symbol $\langle\rangle$ denotes an averaged quantity.

Table I. Measured longitudinal and shear wave velocities and corresponding elastic moduli of Mg-PSZ at damage levels A and D.

Level	Transverse direction					Axial direction				
	C_L mm/μs	C_s mm/μs	ν	E GPa	μ GPa	C_L mm/μs	C_s mm/μs	ν	E GPa	μ GPa
A	7.07	3.71	0.31	205	78.4	6.94	3.64	0.31	198	75.5
D	6.27	3.62	0.25	187	74.7	6.98	3.64	0.31	199	75.5

Equations (1)-(3) can be compared to experimental measurements of the elastic moduli of Mg-PSZ containing axially oriented microcracks. The moduli are determined from the longitudinal and shear wave velocities, C_L and C_S, by

$$\bar{E} = C_L^2 \rho \frac{(1+\bar{\nu})(1-2\bar{\nu})}{(1-\bar{\nu})} \tag{4}$$

$$\bar{\nu} = \frac{1 - 2(C_s/C_L)^2}{2 - 2(C_s/C_L)^2} \tag{5}$$

$$\bar{\mu} = \rho C_s^2 \tag{6}$$

where ρ is the density of the material. The moduli in the directions parallel and transverse to the compression axis are computed from the wave velocities measured in the axial and transverse directions, respectively. These measured velocities and elastic moduli calculated with Eqs.(4)-(6) are listed in Table I.

If microcracking is the major influence on the elastic moduli, then the crack density ε can be estimated from Eqs. (1)-(3) using the moduli listed in Table I. The reduction in Young's modulus at level D requires a crack density ε of about 0.04 and the reduction in shear modulus requires a crack density of 0.03. These values are in approximate agreement with observations of the average size and number of microcracks on the free surface at strain level D, shown in Fig. 3. It may be concluded that changes in ultrasonic velocity and elastic moduli in Mg-PSZ at high levels of inelastic compressive strain are primarily due to the presence of axially oriented microcracks.

ACKNOWLEDGEMENT

This work has been supported by the U.S. Army Research Office under Contract No. DAAL-03-86-K-0169 to the University of California, San Diego.

REFERENCES

1. A.H. Heuer, J. Am. Ceram. Soc. 70(10), 689 (1987).
2. I-W. Chen, J. Am. Ceram. Soc. 69(3), 181-89 (1986).
3. P.F. Follansbee, in Metals Handbook, 9th ed., (American Society for Metals, 1985), Vol. 8, pp. 198-203.
4. S.J. Klima and G. Baaklini, NASA Conf. Pub. 2383, 1986, pp. 117-126.
5. B. Budiansky and R.J.O'Connell, Int. J. Solids Structures, 12,81 (1976).
6. H. Horii and S. Nemat-Nasser, J. Mech. Phys. Solids, 31(2), 155 (1983).
7. S. Nemat-Nasser, Class notes for the course, Micromechanics, University of California, San Diego (1988).